EXCESS NOISE IN GaAs MESFET OSCILLATORS

G. L. Bilbro[1] A. N. Riddle[2] R. J. Trew[1]

[1]North Carolina State University, Raleigh, NC 27695-7911
[2]Macallan Consulting, 1583 Pinewood Way, Milpitas, CA 95035

Abstract

A new technique for numerically simulating oscillator noise spectra is introduced. Additive and multiplicative noise is simulated for three industrial GaAs MESFET designs (with buried-, uniform-, and ion implanted channels) oscillating in simple resonant circuits at a center frequency of $f_0 = 4$ GHz. Each oscillator exhibits excess $1/f$ noise so that $S_\phi(f) \propto f^{-3}$ for small offset frequency f. The simulation predicts that the buried channel oscillator is about 12 dB quieter than oscillators built around either the uniform channel or ion-implanted devices, partly because of differences in device Q's. Using S_ϕ/Q as a figure of merit to account for different Q's, the uniform channel device is 2 dB/Q quieter than the buried channel circuit and about 0.5 dB/Q quieter than the ion-implanted circuit.

1 Introduction

A new and practical technique will be introduced for predicting oscillator noise in terms of the transfer functions of the active device and and the resonant filter comprising the oscillator circuit. The new technique is based on a general theory of oscillator noise suitable for computer analysis of any oscillator[4]. In Section 2, the active device is modeled with a MESFET simulator which combines a physics-based FET model with harmonic balance to predict large-signal RF performance. In Section 3, the resonant filter is determined from conventional oscillator design techniques to maximize power at the load of a simple shunt topology. In Section 4, the inverse transfer function for the entire circuit D is computed from the two component transfer functions. The partial derivatives of D are used to predict the noise spectrum of the oscillator due to upconversion of baseband noise and to crossconversion of inband noise.

Consider the feedback oscillator shown in Figure 1. Let K be the transfer function of the gain network and H be the transfer function of the frequency selective network. The noise response of the oscillator is completely characterized by the inverse transfer function

$$D(a, \omega, e) = 1 - KH \tag{1}$$

a complex function of oscillation amplitude a, frequency ω, and operating conditions e, such as bias voltages[4]. Low frequency variation in the set of parameters e can be upconverted by the oscillator. Although the formulation correctly treats variations in the entire set of e, the present report will restrict itself to noise in the gate bias voltage so that $e \equiv V_g$. The FET operates well into saturation so that variation of drain bias is expected to have little effect on output and is ignored.

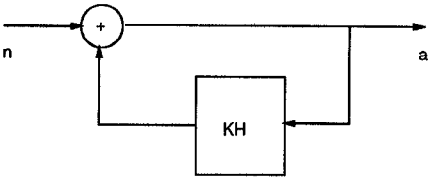

Figure 1: Block diagram of feedback oscillator

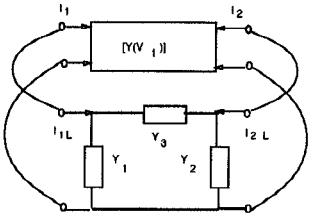

Figure 2: Microwave oscillator. The resonant network is characterized by $Y_k = G_k + jB_k$. The active device is characterized by the parameters $y_{ij} = g_{ij} + jb_{ij}$.

OF1

At microwave frequencies, it is convenient to draw the oscillator circuit as in Figure 2 and to characterize the two-port active GaAs MESFET device with large signal reflection parameters $\hat{S}$ and the passive two-port resonant filter subcircuit including the load with $\tilde{S}$. The inverse transfer function of Equation 1 can be rewritten in terms of $\hat{S}$ and $\tilde{S}$

$$\begin{aligned} D = 1 &- \hat{S}_{21}\tilde{S}_{21} - \tilde{S}_{11}\hat{S}_{22} - \hat{S}_{11}\tilde{S}_{12}\tilde{S}_{21}\hat{S}_{22} \\ &-2\hat{S}_{11}\tilde{S}_{22} - \tilde{S}_{11}\hat{S}_{12}\hat{S}_{21}\tilde{S}_{22} \\ &-\hat{S}_{11}\hat{S}_{12}\tilde{S}_{12}\hat{S}_{21}\tilde{S}_{21}\tilde{S}_{22} + 2\hat{S}_{11}\tilde{S}_{11}\hat{S}_{22}\tilde{S}_{22} \\ &+\hat{S}_{11}^2\tilde{S}_{12}\tilde{S}_{21}\hat{S}_{22}\tilde{S}_{22} + \hat{S}_{11}^2\tilde{S}_{22}^2 \\ &+\hat{S}_{11}\tilde{S}_{11}\hat{S}_{12}\hat{S}_{21}\tilde{S}_{22}^2 - \hat{S}_{11}^2\tilde{S}_{11}\hat{S}_{22}\tilde{S}_{22}^2 \end{aligned} \quad (2)$$

The device parameters $\hat{S}$ depend most strongly on bias and amplitude. The resonant filter is linear so that the filter parameters $\tilde{S}$ depend only on ω.

It is convenient to write inverse transfer function in terms of its real and imaginary parts, $D = U + jV$. The various components of noise can be associated with a corresponding partial derivative as in Table 3, where the partial derivatives are with respect to gate bias V_g, amplitude a, or frequency ω.

2 Determination of Large-Signal $\hat{S}$ Parameters of MESFET

The GaAs MESFET can be characterized with a large-signal physical MESFET model[2] which computes the $\hat{S}$ from device physics and harmonic balance. The model was validated with measured data from industrially-developed experimental transistors. The resulting physical models of the devices were then simulated in a 50 Ohm environment with a 4GHz generator over a range of input powers. In addition, simulations were executed at slightly different values of frequency and gate bias to compute partial derivatives with respect to the variables of interest as in Table 3.

The large-signal MESFET simulations use harmonic balance with harmonics at 8GHz and 12GHz. Simulations with a harmonic at 16GHz were virtually identical, indicating that little error is committed by neglecting harmonics above the third.

The amplitude of oscillation was adjusted to maximize added power produced by each device. S parameters were simulated at that amplitude as shown in Figure 4.

3 Determination of Resonant Filter Parameters $\tilde{S}$

Vehovic *et al.* presented a design procedure for an oscillator of the form shown in Figure 2 using the Y parameters of the active device[5]. In that work, a linear design system was developed whose solution maximized the power delivered to the load and resulted in values for the Y_k of Figure 2 in terms of the y_{ij}. Kotzebue and Parrish extended the procedure[3] and presented closed form solutions for six circuit types including the "first shunt form" shown in Figure 5. More recent procedures address the difficulty of measuring Y parameters at microwave frequencies[1]. However this is not an issue when calculating Y parameters from precisely simulated data.

The result of Kotzebue and Parrish analysis is numerical values of the load conductance g_L, and the three susceptances b_1, b_2, b_3 normalized to $Z_0 = \omega = 1$. The corresponding load resistance is positive and realizable. Positive susceptances correspond to capacitors and the negative susceptances are realized with inductors denormalized with $Z_0 = 50\Omega$ and $\omega = 2\pi \times 4$ GHz.

It is straightforward to calculate the S parameters for the circuit of Figure 5. The real and imaginary parts of the resulting S_{21} are shown in Figure 8 and 9. As expected from oscillator theory, the resonant filter has a peak in its transfer function somewhat lower than the undisturbed resonant frequency of the filter circuit: the real part of $\tilde{S}_{21}$ has an extremum and the imaginary part of $\tilde{S}_{21}$ has a zero just above the specified oscillator center frequency. Since it describes a linear circuit, the filter $\tilde{S}$ are independent of the internal biases in the MESFET and the amplitude of oscillation.

4 Noise Spectra of the Oscillator

The device $\hat{S}$ of Section 2 and the filter $\tilde{S}$ of Section 3 are tabulated at four points that differ by small amount in frequency, power, or gate bias. The frequency interval is 0.1% of the center frequency. The intervals for bias and amplitude are about 10% of the corresponding nominal values. At these points, the inverse transfer function D for the entire oscillator circuit is constructed according to Equation 2. The partials of D with respect to frequency, power, and gate bias are estimated as divided differences. Using the general theory of oscillator noise, the noise spectra for each of the oscillators can be calculated for specificed noise parameters. The results are plotted in Figures 11 and 10 for additive noise $1.0 \times 10^{-9}\ V/\sqrt{Hz}$ and modulation noise $1.0 \times 10^{-9}\ V/\sqrt{Hz}$ with corner frequency $1.0 \times 10^{+7}\ Hz$.

Phase noise spectra are presented in Figure 10. The phase noise spectra for the three oscillators is plotted in Figure 10. The curve for the buried channel device is about 15 dB lower than the corresponding curves for the ion-implanted device or uniform device. From this it can be concluded that the spectral purity of an oscillator based on this buried channel or lo-hi-lo device is significantly better than these ion-implanted or uniform devices.

The amplitude noise spectra for the ion-implanted device is a few decibels lower than the corresponding curves for the uniform and buried channel devices as shown in Figure 11. But the curves of Figure 11 are 100 dB lower than the spectra of Figure 10 so that amplitude noise is negligible compared to phase noise in all the three circuits.

The phase noise for the three oscillators can be normalized to unit Q by dividing by the Qs of the filters, which are 8.8, 6.6, 36.4 for the ion-implanted, uniform, and lo-hi-lo cases. The resulting noise levels of $-68.7, -66.8, -79.5$ dB at 10 kHz, or 0,-0.5,1.5 dB relative to the ion-implanted case.

5 Conclusion

A procedure for noise simulation has been presented for GaAs MESFET oscillators. The procedure integrates a physics-based RF simulation of the active device, conventional oscillator design techniques for the resonant filter, and a general theory of oscillator noise. Electrical characteristics of the active devices are simulated with large-signal MESFET model, which combines the physics of the FET channel with harmonic balance to predict large-signal RF performance. The resonant circuit is determined with conventional oscillator design techniques to maximize power at the load in a simple shunt topology. The inverse transfer function D is computed at four neighboring operating points to estimate partial derivatives of D with respect to frequency, power, and gate bias. These three partials are used to predict noise due to upconversion of baseband noise and to crossconversion of inband noise.

Three transistor designs were simulated: an ion-implanted device, a uniform channel device, and a buried-channel or lo-hi-lo device. For each, baseband noise on the gate bias was considered and its effect was reflected in the phase noise spectrum $S_\phi(f)$ as excess $1/f$ noise near the center frequency $f < f_c$, where f_c is the corner frequency and derives from the spectrum of the baseband noise. The phase noise spectrum $S_\phi(f)$ $S_\phi(f) \propto f^{-3}$ near f_0 and $S_\phi(f) \propto f^{-2}$ further away, but the curve is 13 dB lower for the buried channel device. The amplitude noise spectra for the devices differ by about 5 dB but are 100 dB lower than phase noise.

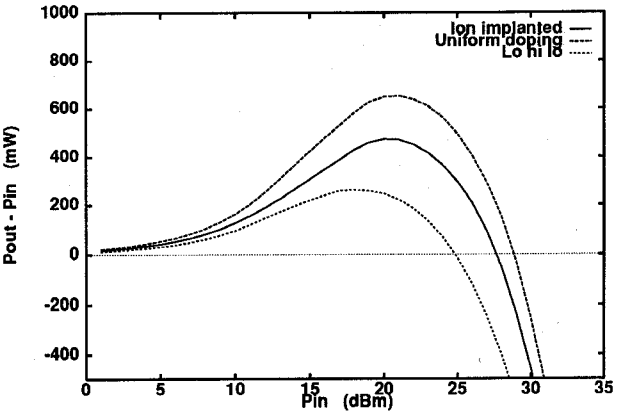

Figure 4: Added power as a function of input power in for the three devices.

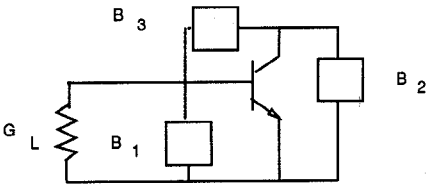

Figure 5: First shunt form of resonant circuit as realized in Kotzebue *et al.*

Partial of D	Conversion Effect
$\partial U/\partial V_g$	Baseband to AM upconversion
$\partial V/\partial V_g$	Baseband to PM upconversion
$\partial V/\partial a$	AM to PM crossconversion
$\partial U/\partial \omega$	PM to AM crossconversion
$\partial V/\partial \omega$	PM to PM
$\partial U/\partial a$	AM to AM

Figure 3: Correspondences between noise conversion modalities and partial derivatives of the inverse transfer function $D = U + jV$ with respect to gate bias, amplitude, and frequency.

References

[1] R. J. Gilmore and F. J. Rosenbaum. An analytic approach to optimum oscillator design using s-parameters. *IEEE Trans. MTT*, MTT-31:633–639, 1983.

[2] M. A. Khatibzadeh and R. J. Trew. A large-signal, analytic model for the GaAs MESFET. *IEEE Trans. Microwave Theory and Techniques*, MTT-36:231–238, 1988.

[3] K. L. Kotzebue and W. J. Parrish. The use of large signal s-parameters in microwave oscillator design. In *Proc 1975 IEEE Intl. Symp. Circuits and Systems*, 1975.

[4] A. N. Riddle. *Oscillator noise: theory and characterization.* PhD thesis, North Carolina State University, 1986.

[5] M. Vehovic, L. Houselander, and R. Spence. On oscillator design for maximum power. *IEEE Trans. Circuit theory*, CT-15:281–283, 1968.

Device		Susceptances		
	g_L	b_1	b_2	b_3
Ion impl.	7.09	39.83	26.02	-16.39
Uniform	6.35	25.72	17.71	-10.92
Lo hi lo	10.10	-257.0	-86.9	64.15

Figure 6: Normalized numerical values of susceptances of Figure 5 for the optimal resonant circuit for the ion-implanted FET.

Device		Immittances		
	R_L	1	2	3
Ion impl.	7.06 Ω	3.17E-11 F	2.07E-11 F	1.21E-10 H
Uniform	7.88 Ω	2.05E-11 F	1.41E-11 F	1.82E-10 H
Lo hi lo	4.95 Ω	7.74E-12 H	2.29E-11 H	5.10E-11 F

Figure 7: Physcial values of elements corresponding to the normalized values of Figure 6 with $Z_0 = 50\Omega$ and $\omega = 2\pi \times 4GHz$.

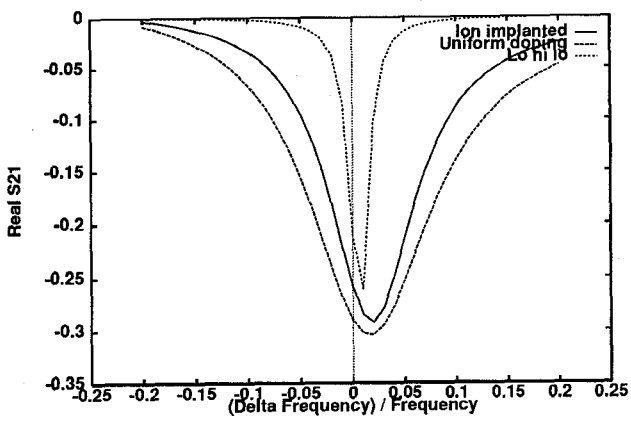

Figure 8: Real part of S_{21} for the optimal resonant filters at 4 GHz.

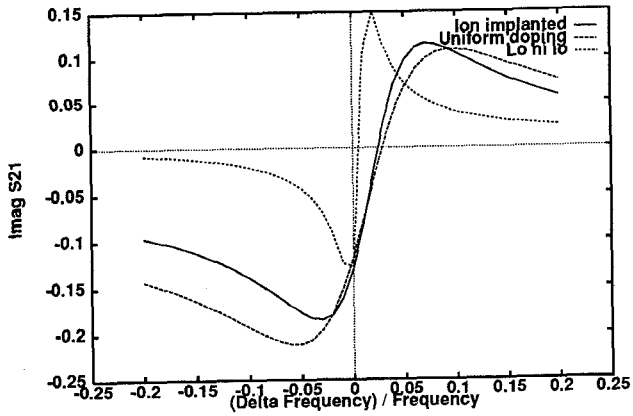

Figure 9: Imaginary part of S_{21} for the optimal resonant filters at 4 GHz.

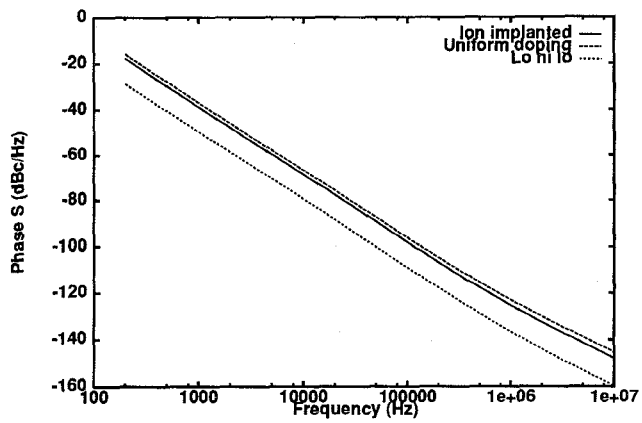

Figure 10: Phase noise spectrum of oscillator output.

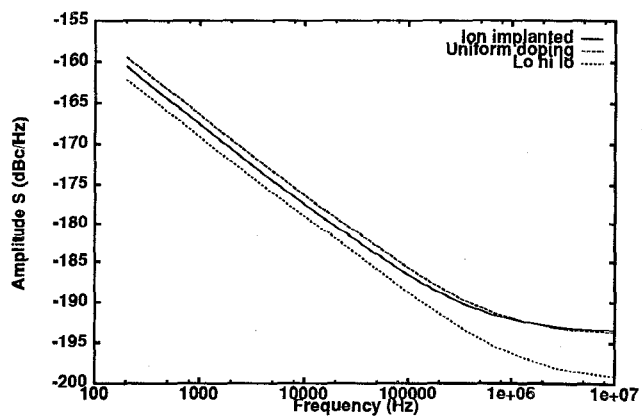

Figure 11: Amplitude noise spectrum of oscillator output.